Study on nanodispersion of PI/clay nanocomposite by *temporal analyses*

Hsueh-Shih Chen*, Chien-Ming Chen, Gwo-Yang Chang, Shyh-Yang Lee

*Organic-Inorganic Hybrid Laboratory, Union Chemical Laboratories, Industrial Technology Research Institute,
321 Kuang-Fu Road Section 2, Hsinchu City 300, Taiwan, ROC*

Abstract

The detail of nanoscaled dispersive behavior for layered clay in polyimide was first illustrated using *temporal analyses*. The layered structure of pristine clay remained in the poly(amic acid) and polyimide matrixes almost throughout curing process. However, the clay was mutilated by polymer chain motion during the process (cluster size reduced from ∼700 to ∼298 nm). On the other hand, organo-clay modified with octadecyldimethyl (3-trimethoxysilylpropyl) ammonium chloride initially exfoliated in the poly(amic acid) solution (d-spacing >42 nm). At room temperature ∼200 °C, the layered structure of the clay recovered due to loss of solvent and poly(amic acid) chains intercalating into the organo-clay interlayer ($d \sim 3.49$ nm). After polyimide fully formed at 350 °C, organo-clay d-spacing decreased to ∼2.27 nm. The reduction of d-spacing was ascribed to some of the polyimide molecular chains being squeezed out of the organo-clay interlayer since hydrogen bonds between the organo-clay and poly(amic acid) molecules diminished. The change in organo-clay cluster size behaved like pristine clay, finally decreasing to ∼367 nm after polyimide formed completely. The relatively large size of the organo-clay clusters in polyimide was ascribed to the confinement effect of polymer chain motion by organo-clay since the chains were frozen in the organo-clay interlayer.
© 2005 Elsevier B.V. All rights reserved.

Keywords: Composite materials; Nanostructures; Polymers; Thin films

1. Introduction

Polyimide/clay nanocomposite has attracted strong interest from researchers over the past decade [1–3]. The microstructure and dispersivity of clay in the polyimide matrix dominates polyimide/clay nanocomposite performance. Pristine clay is hydrophilic, accounting for why various surfactants have been used as intercalants to increase the clay d-spacing and modify it into hydrophobic organoclay, making it compatible with polyimide [4]. Studies have shown that polyimide properties can be greatly improved by introducing clay into polyimide matrixes [1–10].

Layered clay is a native mineral consisting of two fused silica tetrahedral slabs between which are edge-sharing octahedral 1-nm thick nanoslabs of alumina and/or magnesia. Substituting Si^{4+} for Al^{3+} or Al^{3+} for Mg^{2+} in the lattice generates an excess of negative charges in the clay interlayer. Accordingly, the nanoslabs absorb some cations, such as Li^+ or Ca^{2+}, to balance the charge disequilibrium in the interlayer.

Most reports to date have claimed that organo-clay cannot fully exfoliate in a polyimide matrix. This failure was attributed to the poor affinity of organo-clay for the polyimide matrix, i.e., a strong bond cannot form between the clay and polyimide molecules. To the best of the authors' knowledge, the affinity is determined by the forces of interaction, including covalent bonding, hydrogen bonding, and van der Waals force among clay, solvent molecules and polymer chains, which influencing the dispersivity of the clay in the polyimide matrix.

In the conventional view, organo-clay exfoliation or intercalation in a specific polymer depends on its d-spacing or intercalant. However, it ignores the effect of molecular interaction during the polymerization. Actually molecular interactions among clay, solvent, and polymer, vary during polymerization or imidization since the composite composition

* Corresponding author. Tel.: +886 3 5743941; fax: +886 3 573 2347.
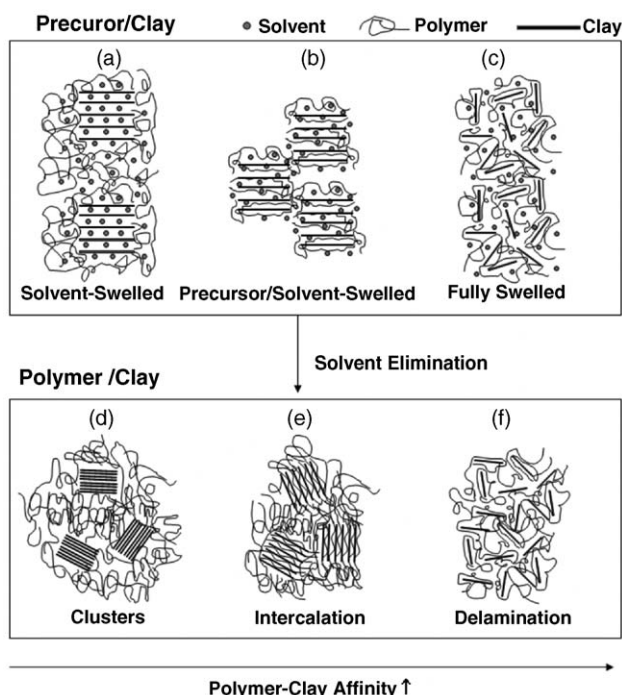 *E-mail address:* sean@itri.org.tw (H.-S. Chen).

Fig. 1. Morphologies of clay dispersed in a polymer. The affinity of clay for a polymer is determined by interactions such as hydrogen bonding or permanent dipole moment between the polymer chains and the clay nanoslabs.

or molecular structure always changes. Therefore, considering interactions among the composite components rather than only noting intercalant type seems to be better for designing a well-dispersed nanocomposite. Fig. 1 shows three possible cases of polymer/clay composite dispersion dependent on molecular interactions among precursor molecules, solvent, and clay.

In this work, we depict the dispersion behaviors of clay in polyimide during the preparation process by means of *temporal analyses*, including of X-ray diffraction (XRD), thermo-gravimetric analysis (TGA) and transmission electron microscopy (TEM).

2. Experimental

Na-montmorillonite (layered clay) with a CEC of 76 meq/100 g was supplied by Pai Kong Co., Ltd. The clay was dried at 80 °C for 3 h before use. The intercalant (surfactant) used was octadecyldimethyl (3-trimethoxysilylpropyl) ammonium chloride (60% in methanol) purchased from Gelest, as sketched in Fig. 2a. Pyromellitic dianhydride (PMDA, 98%) and 4,4′-oxydianiline (ODA, 98%) were obtained from Chriskev, and *N,N*-dimethylacetamide (DMAC, b.p. = 164–166 °C, 99.97%) was purchased from Tedia. PMDA was dried at 150 °C for 3 h before use.

The polyimide precursor, poly(amic acid) (PAA) was obtained by polymerization from 1.1 g of PMDA and 1.0 g of ODA in 11.1 g of DMAC in nitrogen at room temperature. The apparent viscosity of the PAA, as measured by Brookfield, was approximately 7000 cps at 30 °C. The inherent viscosity was 1.12 dl/g (0.5 g/dl in DMAC at 30 °C).

Pristine hydrophilic clay was modified with intercalant using cation-exchange method. 10 g of clay and 11.4 mmol of octadecyldimethyl(3-trimethoxysilylpropyl)ammonium chloride were dissolved in 1000 ml of 0.01N HCl solution. After stirring at 80 °C for 12 h in darkness, the suspension was washed in hot distilled water several times to remove residual chloride or cations. The suspension was then filtered and dried in a vacuum at 80 °C for 24 h. The dried cake was milled and sieved, and white powder was thus obtained. The organophilic modified layered clay was organo-clay. Details of this synthesis and the characteristics of this nanocomposite will be published elsewhere.

The PAA/organo-clay solution was prepared by mixing sufficient amounts of organo-clay and PAA solution for 3 h in argon. The suspension was then placed in a desiccator filled with argon overnight to remove gas bubbles. The solution was coated on glass to a thickness of 200 μm using an automatic coater at a linear speed of 0.8 cm/s. PI/organo-clay films were obtained by curing wet PAA/organo-clay films at 100 °C for 10 min, 160 °C for 20 min, and 350 °C for 120 min in a circulation oven in air at a heating rate of 4 °C/min. After curing, ∼18 μm light yellowish thin-films were obtained.

XRD spectra were obtained using XD-D1 Shimadzu X-ray Diffractometer with Cu Kα radiation (1.54 nm) at 40 kV/35 mA. Clay *d*-spacing was determined using Bragg's equation. The average cluster sizes of clay in PAA or PI matrixes were estimated by applying Schrrer's formula.

$$D = \frac{0.9\lambda}{\beta_{1/2} \cos \theta_B} \tag{1}$$

where D represents the average cluster size, λ is the wavelength of Cu Kα, $\beta_{1/2}$ is the FWHM (full-width at half-maximum), and θ_B is the diffraction angle.

Microstructure and morphology of the specimens were analyzed using TEM (Hitachi 7500 transmission electron microscope) operating at 100 kV. A piece of the specimen was encapsulated in epoxy and cured. The cured specimen was sectioned into thin slices using a microtome with a diamond knife. Carbon was then deposited onto the slices for TEM observation.

Seven specimens were placed in an oven for *temporal investigation* of structural changes in the PI/clay nanocomposite during the curing process. Upon removal from oven, the specimens were instantly cooled in a refrigerator (∼5 °C) to stop the reaction at selected time intervals, as shown in Fig. 3. The specimens were analyzed using XRD and TEM. *Temporal weight losses* following the same heating history were determined via TGA (Du-Pont TA-Q500), using the precursor solution (PAA/clay/DAMC) directly. A heating rate of 4 °C/min was used for these processes.
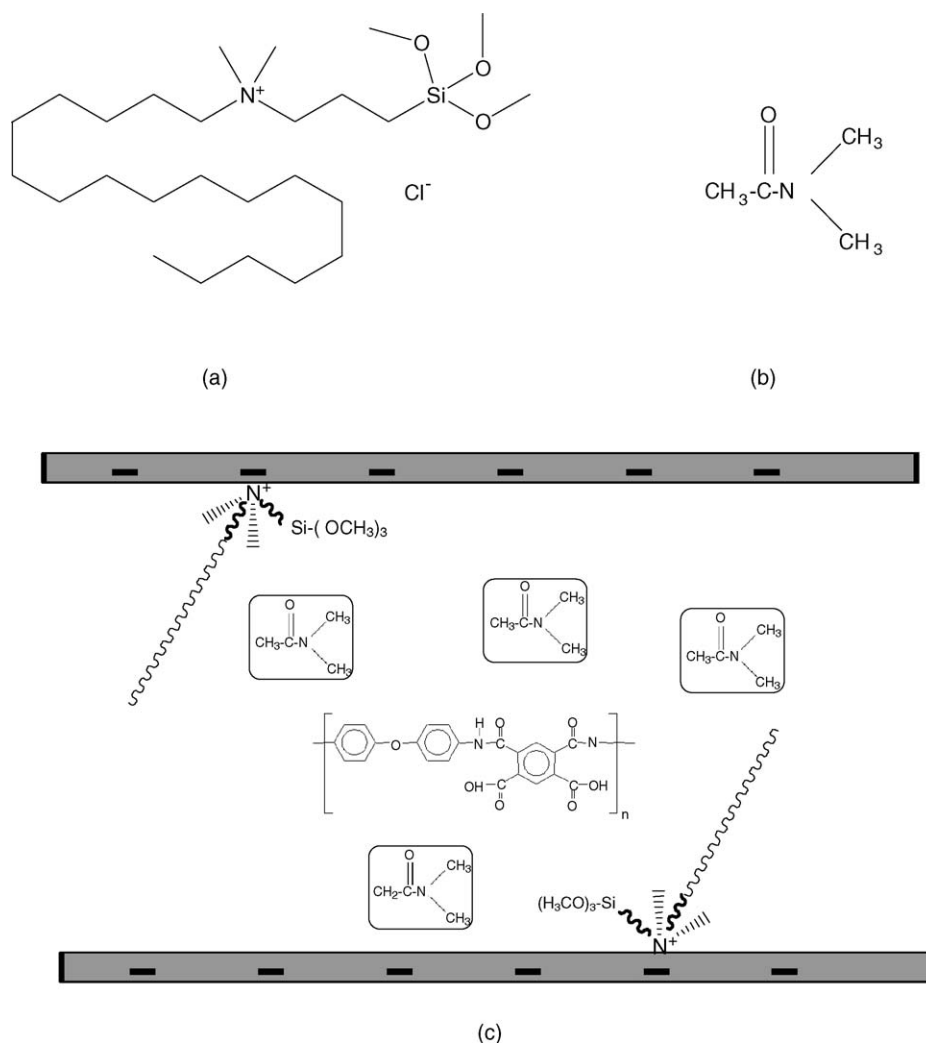
Fig. 2. (a) Organo-clay intercalant: octadecyldimethyl(3-trimethoxysilylpropyl)ammonium chloride ($C_{26}H_{58}ClNO_3Si$); (b) *N,N*-Dimethylacetamide (DMAC) was used as a solvent to swell the organo-clay; (c) a mixture of poly(amic acid), DMAC solvent and organo-clay. Poly(amic acid) was synthesized in DMAC and mixed with clay/DMAC solution. Hydrogen bonds or dipole–dipole interactions forms therein.
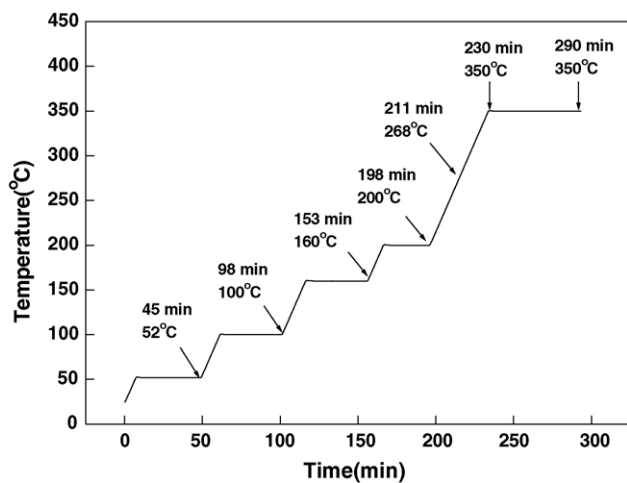

Fig. 3. Heating history of the specimens. Typically, the imidization of polyimide from precursor occurred at ∼200 °C.

3. Results and discussion

Fig. 4a and b show the respective PI/clay and PI/organo-clay XRD patterns. The clay and organo-clay *d*-spacings are ∼1.29 nm ($2\theta = 6.82°$) and ∼4.01 nm ($2\theta = 2.2°$), respectively. Clearly, the intercalant was inserted into the organo-clay interlayers since their *d*-spacing increased. Diffraction peaks for polyimide/clay nanocomposite with higher clay content (3, 5, 7 and 10 phr), appeared at about $2\theta = 6.5°$, indicating the *d*-spacing of clustered clay did not change obviously, as shown in Fig. 4a. No diffraction peaks are observed at lower clay content (3 phr <), suggesting that clay nanoslabs exfoliated in a polyimide matrix only at low concentrations. However, the TEM images show that the clay still retained its layered structure in the polyimide matrix (not shown). Since XRD peak intensity corresponds to the scattering volume of layered clay in a polyimide matrix, weak peak intensity could be expected for nanocomposite with low clay content. In other words, the lack of XRD peaks suggests the XRD
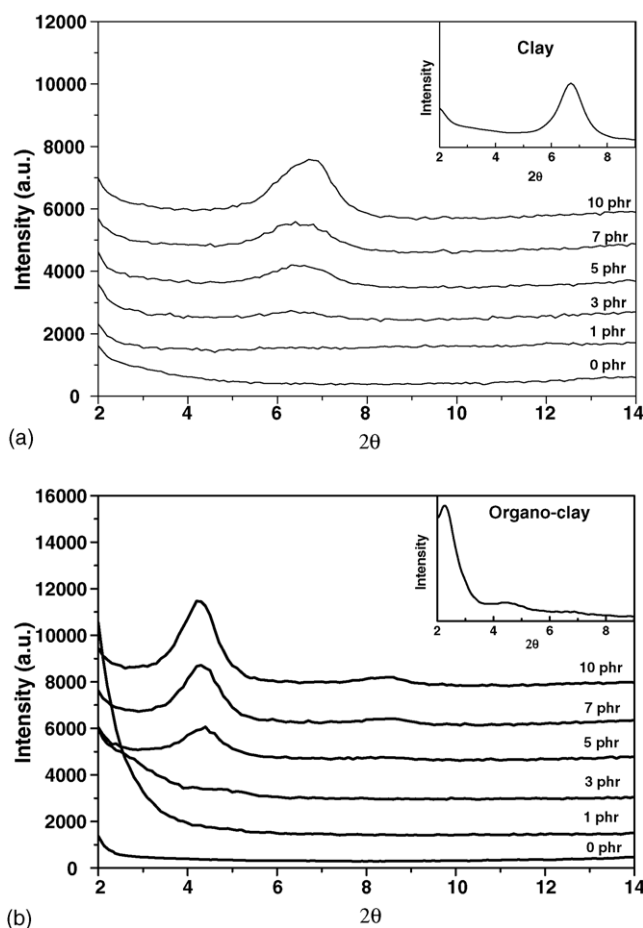
Fig. 4. XRD of the PI/clay film (a) and the PI/organo-clay film (b). The insets show clay and organo-clay spectra, respectively. PI film was obtained by converting PAA solution via thermal curing process.
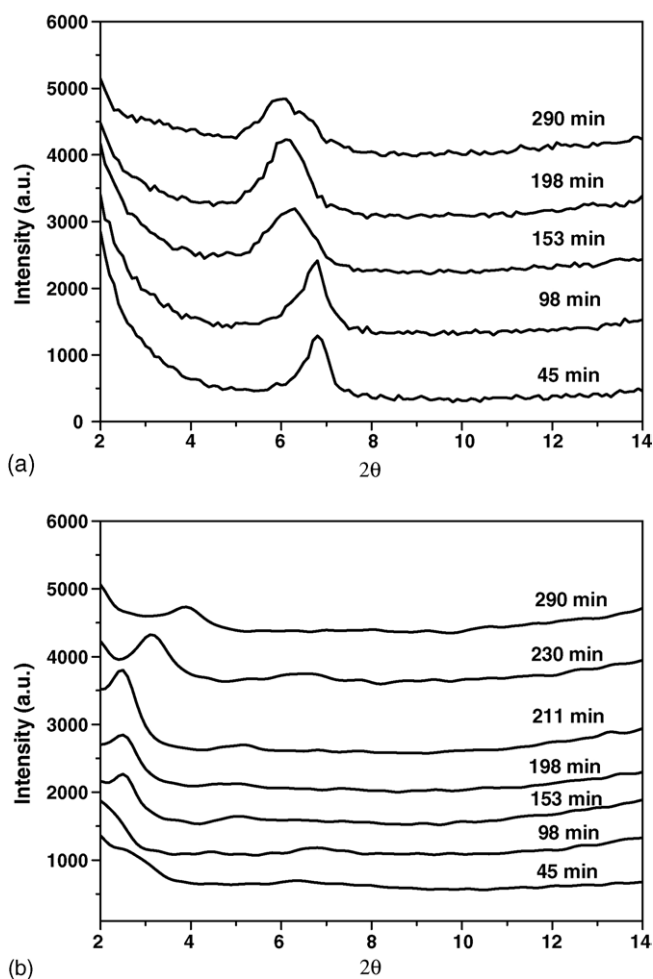

Fig. 5. Temporal XRD spectra of PI/clay film (a) and PI/organo-clay film (b) cured for different durations. The samples were coated on glass substrates and cured in a circulation oven. The clay content of the samples was 3 phr.

detector just did not collect enough signals, contrary to the conventional view that clay disperses well and exfoliates at lower concentrations.

The PI/organo-clay yielded a different outcome. Diffraction peaks at $2\theta = 4.3°$, corresponding to a d-spacing of 2.05 nm, suggest that polyimide chains intercalated into the clay interlayer, as shown in Fig. 4b. At higher clay concentrations (>5 phr), the relative diffraction peak intensities of PI/organo-clay were greater than those of PI/clay. This indicates that at higher concentrations organo-clay has a more regular layered structure than pristine clay in the PI matrix. The diffraction peak of 3-phr PI/organo-clay is not obvious, implying a layered structure did not exist or was so perturbed by chain motion that the signal collected was below the detector sensitivity.

XRD *temporal analysis* of 3-phr PI/clay during the curing process is shown in Fig. 5a. The peak position of pristine clay changed from 6.76 to 6.01° (a d-spacing changed from 1.31 to 1.47 nm) after PI formation, which shows that the clay structure was retained almost throughout the process.

On the other hand, the peak position of organo-clay varied greatly during the curing process, as shown in Fig. 5b.

At 52 °C, the 2θ of the peak was less than 2° (d-spacing ~4.41 nm), indicating the organo-clay exfoliated (or d-spacing exceeded 4.41 nm). When the temperature was increased to 160 °C, the peak shifted to ~2.5° (d-spacing ~3.54 nm), implying the layered structure recovered. The d-spacing of the organo-clay decreased further (~2.80 nm) as the temperature increased to 350 °C. After cured at 350 °C for another 1 h to ensure complete imidization, the final d-spacing was 2.27 nm. Trends of weight, cluster size, and d-spacing change for PI/clay or PI/organo-clay during the curing process are shown in Fig. 6a and b. The data are summarized in Tables 1 and 2.

Because pristine clay is hydrophilic, it is incompatible with the hydrophobic polymer. Hence the clay nanoslabs cannot delaminate or disperse into the hydrophobic polymer matrix. As Fig. 6a shows, the d-spacing did not change significantly during the process. However, the clay cluster size was ~700 nm initially and decreased to ~300 nm in the polymer matrix. This result suggests the clay clusters were gradually mutilated by polymer chain motion during the curing process

although there was no significant intercalation between the clay and the polymer.

Hydrophobic organo-clay had a strong affinity for the PAA solution due to the hydrogen bonds between the organo-clay and precursor solution so it exfoliated in the PAA solution at 52 °C, as shown in Fig. 2c. The solid content of the PI/organo-clay precursor solution (∼34.66% at 52 °C) was also higher than that of the PI/clay precursor solution (∼13.71% at
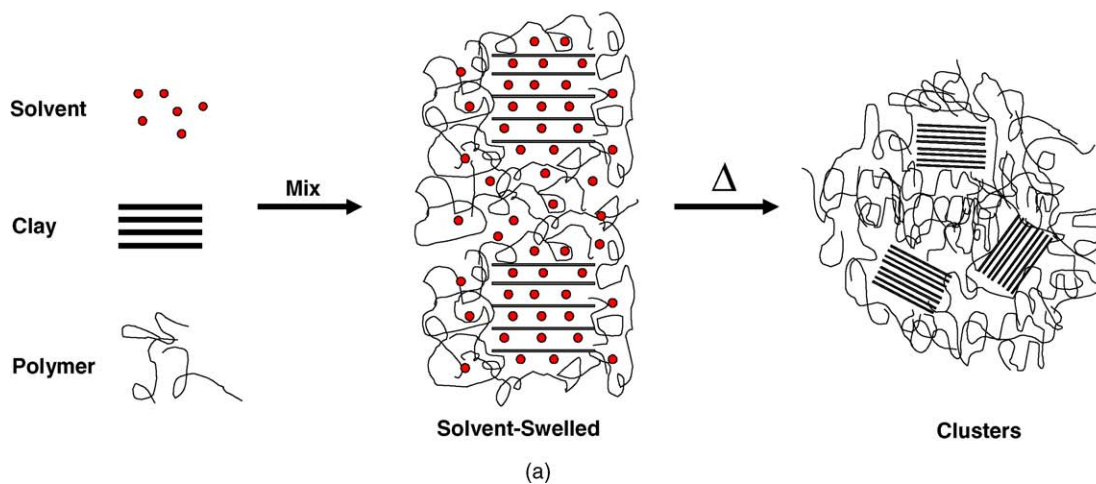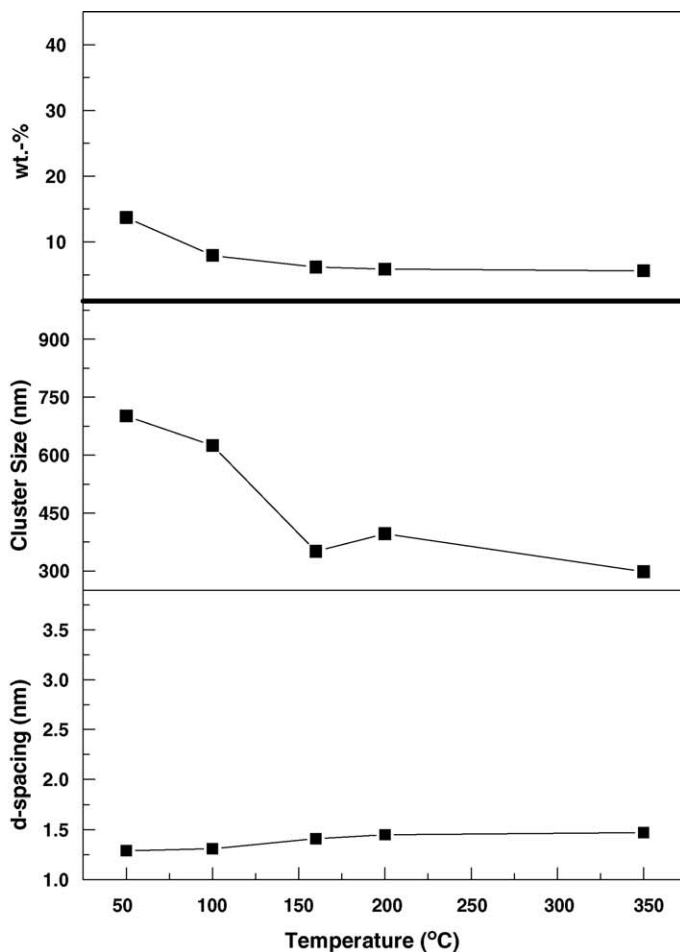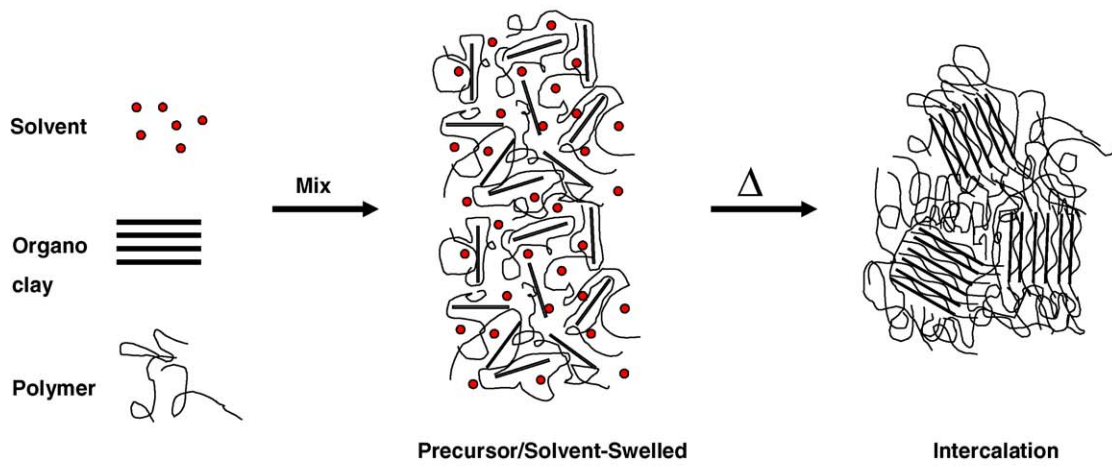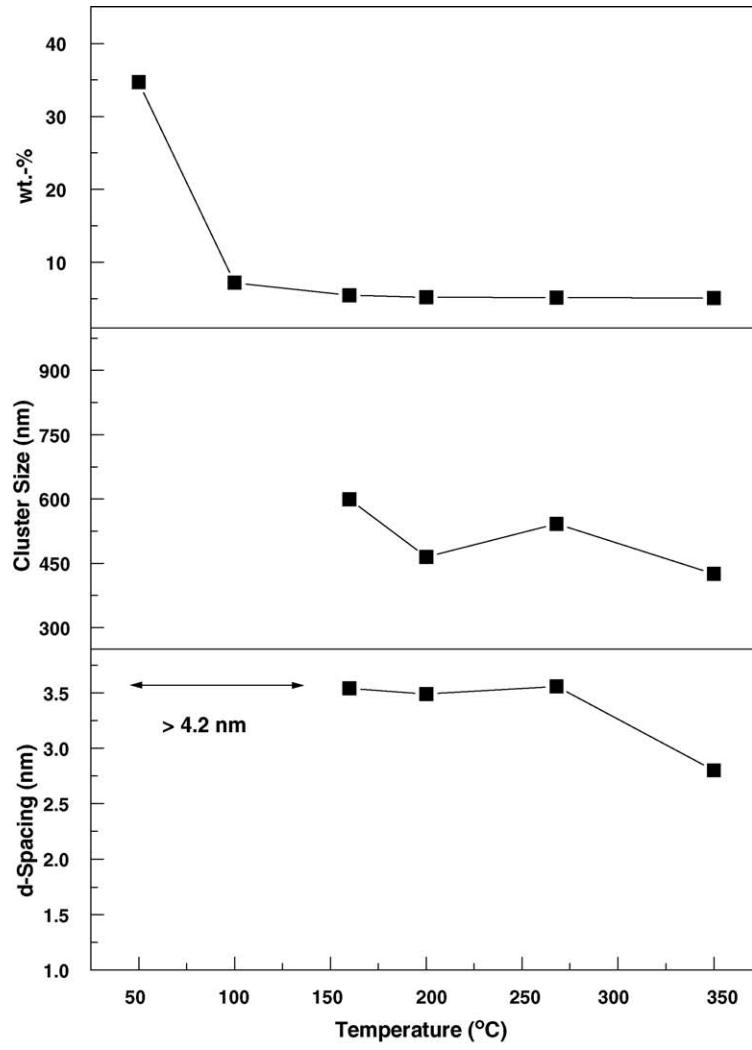

Fig. 6. Trends of weight, average cluster size, and *d*-spacing changes for 3-phr PI/clay (a) and 3-phr PI/organo-clay (b) during curing. The investigation was carried out from 52 to 350 °C, i.e., from PAA to PI.
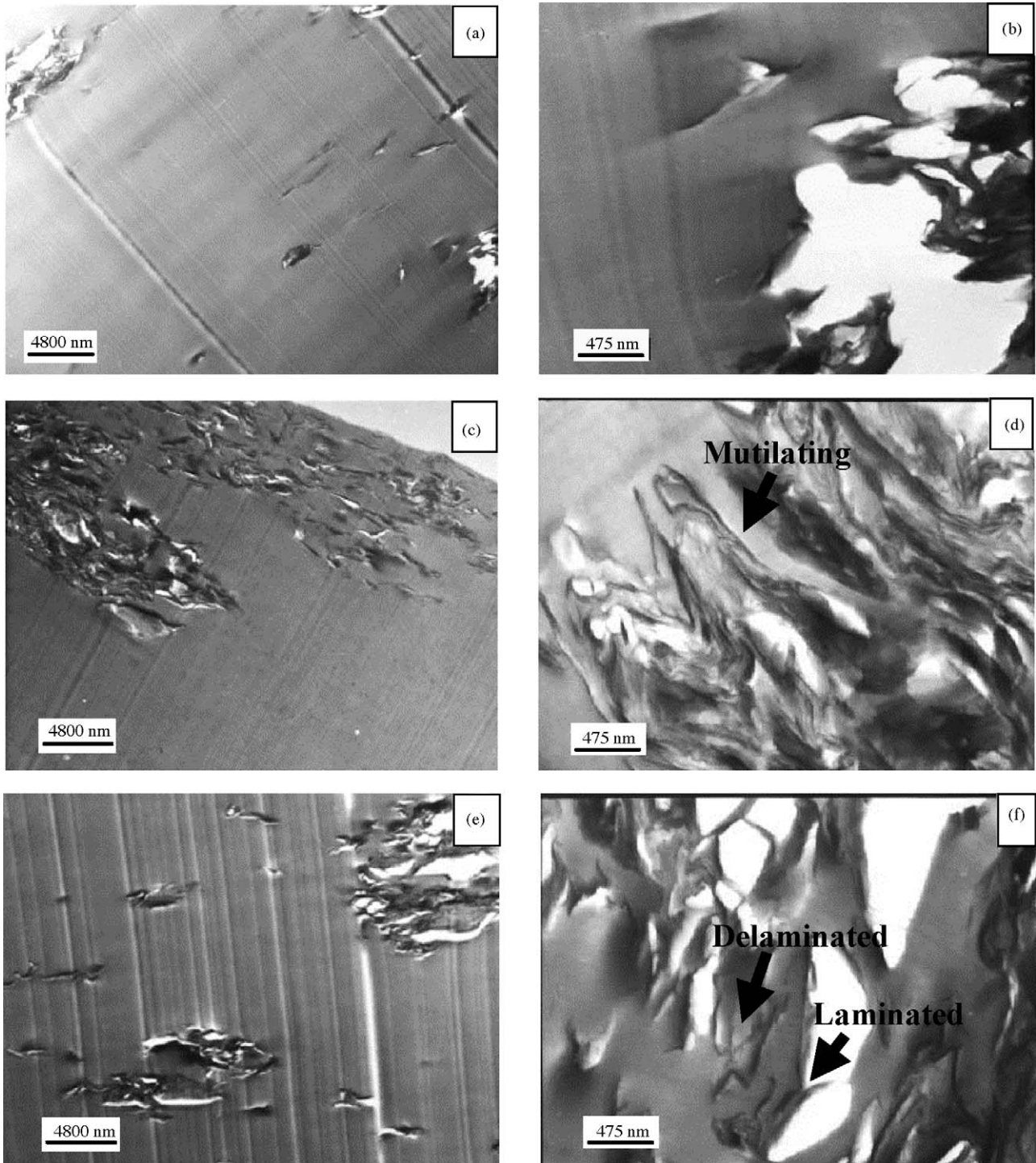
(b)

Fig. 6. (*Continued*).

Fig. 7. TEM images of 3-phr PI/organo-clay films cured at 100 °C (a and b), 200 °C (c and d), and 350 °C (e and f).

52 °C). This implies that the binding force between the solvent and the organo-clay was stronger than that between the solvent and the pristine clay. As the temperature was increased to ~200 °C, the organo-clay d-spacing decreased to ~3.49 nm. Because most of the solvent had been removed from the PAA matrix at ~200 °C, the increase in organo-clay d-spacing in this situation was attributed to intercalated PAA molecules.

PI imidization starts at approximately 200 °C and completes at ~300 °C in ~1 h [11]. Interestingly, in the 200–268 °C range, the d-spacing increased slightly from 3.49 to 3.56 nm, indicating that transforming molecular

Table 1
Temporal XRD and *temporal* TGA data for 3-phr PI/clay

Time (min)	Temperature (°C)	Weight of specimen (%)	2θ (°)	d-spacing (nm)	FWHM (°)	Average cluster size (nm)
45	52	13.71	6.76	1.31	0.65	701.5
98	100	7.93	6.74	1.31	0.73	624.6
153	160	6.16	6.24	1.41	1.30	350.6
198	200	5.86	6.09	1.45	1.15	396.3
211	268	5.79	–	–	–	–
230	350	5.72	–	–	–	–
290	350	5.61	6.01	1.47	1.53	297.9

Table 2
Temporal XRD and *temporal* TGA data of 3-phr PI/organo-clay

Time (min)	Temperature (°C)	Weight of specimen (%)	2θ (°)	d-spacing (nm)	FWHM (°)	Average cluster size (nm)
45	52	34.66	–	–	–	–
98	100	7.20	–	–	–	–
153	160	5.48	2.49	3.54	0.76	599.0
198	200	5.22	2.53	3.49	0.98	464.6
211	268	5.16	2.48	3.56	0.84	542.0
230	350	5.12	3.15	2.80	1.07	425.5
290	350	5.06	3.88	2.27	1.24	367.3

chains expanded the organo-clay interlayer during PI formation. However, the hydrogen bonds between the organo-clay and PAA decreased gradually during PI formation, resulting in a decrease in affinity. As PAA formed PI at 350 °C, the d-spacing decreased to 2.27 nm. This result was ascribed to some polyimide molecular chains being squeezed out of the interlayer. Hence, variation in affinity determined clay dispersion behavior in the polyimide matrix. On the other hand, the change in cluster size of organo-clay behaved like that of pristine clay: the cluster size was gradually reduced during PI formation. However, the final cluster size of organo-clay ($\sim$367 nm) was larger than that of pristine clay ($\sim$298 nm), which could be attributed to confinement of the polymer chains by organo-clay since they were frozen inside the organo-clay interlayer.

TEM images of PI/organo-clay support the above results. The organo-clay clustered at 100 °C (>600 nm), as shown in Fig. 7a and b. Besides clusters, few sheets of organo-clay are found in the matrix. At 200 °C, the layered structure of organo-clay became irregular, as shown in Fig. 7c and d. XRD shows that the d-spacing and clusters size fluctuated slightly during this stage so the organo-clay should have been being mutilated by polymer chains. When the temperature was increased to 350 °C, polyimide formed completely. The organo-clay further separated into smaller clusters with a layered structure. Moreover, some sheets were delaminated, as shown in Fig. 7e and f.

Based on the results presented above, the dispersion behavior can be described follows. The organo-clay first exfoliated in the precursor solution at room temperature, recovered when the solvent evaporated at higher temperatures, and was intercalated by PI chains while they were mutilated by chain motion throughout the process.

4. Conclusion

To summarize, we have illustrated the nanoscaled dispersion behaviors of layered clay in polyimide using *temporal analyses*. The layered structure of pristine clay was retained in poly(amic acid) and polyimide matrixes during curing while the clusters were mutilated (from $\sim$700 to $\sim$298 nm) by polymer chain motion during the process. On the other hand, organo-clay modified with octadecyldimethyl (3-trimethoxysilylpropyl) ammonium chloride initially exfoliated in the poly(amic acid) solution (d-spacing >42 nm). At room temperature $\sim$200 °C, the loss of solvent resulted a recovery of the clay layered structure ($d \sim 3.49$ nm). The increase in d-spacing is ascribed to intercalation of poly(amic acid) chains in the organo-clay interlayer. From 200 to 268 °C, the poly(amic acid) began imidizing to polyimide and the transforming molecules expanded d-spacing of the organo-clay interlayer slightly ($d \sim 3.56$ nm). Finally, as polyimide fully formed at 350 °C d-spacing decreased again ($d \sim 2.27$ nm), which is ascribed to some polyimide chains being squeezed out of interlayer due to reduction of hydrogen bonds between the organo-clay and the poly(amic acid). The change in cluster size of organo-clay behaved like pristine clay, finally decreasing to $\sim$367 nm after polyimide formation. The relatively large cluster size of the organo-clay in polyimide is ascribed to the confinement effect of polymer chain motion by organo-clay since the chains were frozen in the organo-clay interlayer.

References

[1] A. Gu, S.W. Kuo, F.C. Chang, J. Appl. Polym. Sci. 79 (2001) 1902.

[2] A. Gu, S.W. Kuo, F.C. Chang, J. Appl. Polym. Sci. 79 (2001) 289.

[3] H.L. Tyan, Y.C. Liu, K.H. Wei, Chem. Mater. 11 (1999) 1942.

[4] K. Yano, A. Usuki, T. Kurauchi, O. Kamigaito, J. Polym. Sci. Part: Polym. Chem. 31 (1993) 2493.

[5] H.L. Tyan, Y.C. Liu, K.H. Wei, Polymer 40 (1999) 4877.

[6] Y. Yang, Z.K. Zhu, J. Yin, X.Y. Wang, Z.E. Qi, Polymer 40 (1999) 4407.

[7] K. Yano, A. Usuki, A. Okada, J. Polym. Sci. A 35 (1997) 2289.

[8] A. Gu, F.C. Chang, J. Appl. Polym. Sci. 79 (2001) 289.

[9] S.H. Hsaio, G.S. Liou, L.M. Chang, J. Appl. Polym. Sci. 80 (2001) 2067.

[10] P.C. LeBaron, Z.T. Wang, Pinnavaia, J. Appl. Clay Sci. 15 (1999) 11.

[11] K.G. Malay, K.L. Mittal, Polyimides: Fundamentals and Applications, Marcel Dekker, New York, 1996, p.15.